HHS Public Access

Author manuscript

Virology. Author manuscript; available in PMC 2019 May 01.

Published in final edited form as:

Virology. 2018 May ; 518: 385–397. doi:10.1016/j.virol.2018.03.018.

Genomic, Recombinational and Phylogenetic Characterization of Global Feline Herpesvirus 1 Isolates

Andrew C Lewin[a,b,*], **Aaron W. Kolb**[c,*], **Gillian J. McLellan**[a,b,c], **Ellison Bentley**[a,b], **Kristen A. Bernard**[d], **Sandra P. Newbury**[e], and **Curtis R. Brandt**[b,c,f,#]

[a]Department of Surgical Sciences, School of Veterinary Medicine, University of Wisconsin-Madison, Wisconsin, USA

[b]McPherson Eye Research Institute, University of Wisconsin-Madison, Wisconsin, USA

[c]Department of Ophthalmology and Visual Sciences, School of Medicine and Public Health, University of Wisconsin-Madison, Wisconsin, USA

[d]Department of Pathobiological Sciences, School of Veterinary Medicine, University of Wisconsin-Madison, Wisconsin, USA

[e]Department of Medical Sciences, School of Veterinary Medicine, University of Wisconsin-Madison, Wisconsin, USA

[f]Department of Medical Microbiology and Immunology, School of Medicine and Public Health, University of Wisconsin-Madison, Wisconsin, USA

Abstract

Feline herpes virus type 1 (FHV-1) is widely considered to be the leading cause of ocular disease in cats and has been implicated in upper respiratory tract infections. Little, however is known about interstrain phylogenetic relationships, and details of the genomic structure. For the present study, twenty-six FHV-1 isolates from different cats in animal shelters were collected from eight separate locations in the USA, and the genomes sequenced. Genomic characterization of these isolates including short sequence repeat (SSR) detection, with fewer SSRs detected, compared to herpes simplex viruses type 1 and 2. For phylogenetic and recombination analysis, 27 previously sequenced isolates of FHV-1 were combined with the 26 strains sequenced for the present study. The overall genomic interstrain genetic distance between all available isolates was 0.093%. Phylogenetic analysis identified four main FHV-1 clades primarily corresponding to geographical collection site. Recombination analysis suggested that interclade recombination has occurred.

[#]Address correspondence to Curtis R. Brandt, PhD, 550A Bardeen Medical Laboratory, 1300 University Ave., Madison, WI 53706. USA, (608) 262-8054, crbrandt@wisc.edu.

[*]These authors contributed equally to this project.

Conflict of interest statements

The authors declared no potential conflicts of interest with respect to the research, authorship, and/or publication of this article.

Keywords

feline herpesvirus; herpes; varicellovirus; genome sequencing; veterinary; ocular; phylogenetics; recombination

1. Introduction

Feline herpes virus type 1 (FHV-1) is widely considered to be the leading cause of conjunctival and corneal ulceration in cats (Hartley, 2010) and has been implicated in upper respiratory tract infections as well as a variety of painful ocular conditions including ulcerative keratitis, corneal sequestra, eosinophilic conjunctivitis, uveitis and keratoconjunctivitis sicca (Gaskell et al., 2007). Serological studies indicate that up to 97% of cats have been exposed to the virus (Maggs and Clarke, 2005). More than 80% of cats will become persistently infected following exposure, and 45% will shed virus in response to stressful stimuli (Gaskell and Povey, 1977). The clinical signs of FHV-1 on initial exposure frequently include conjunctivitis, keratitis and upper respiratory disease. This phase is often self-limiting but can result in permanent corneal scarring and symblepharon formation with subsequent blindness (Gould, 2011). Three FHV-1 vaccines are commonly used in the USA, and these are combined with vaccines against feline calicivirus (FCV), and feline panleukopenia virus (FPV) (Reagan et al., 2014). Vaccination against FHV-1 is recommended for all cats, especially young animals in high risk settings, however reduced protection is possible upon intense challenge, and the vaccine will not prevent infection (Thiry et al., 2009).

Although earlier work suggested that FHV-1 was serologically homogeneous (Gaskell and Willoughby, 1999), there have been more recent reports describing differences between isolates identified using PCR techniques. These studies examined the genetic differences between FHV-1 isolates using restriction endonuclease digest to cleave viral DNA (Hamano et al., 2005), and strain differences in viral glycoprotein expression (Hamano et al., 2004). Other papers have evaluated, examined or sequenced smaller individual components of the FHV-1 genome (Hara et al., 1996; Herrmann et al., 1984; Kawaguchi et al., 1994; Maeda et al., 1992; Maeda et al., 1993; Maeda et al., 1995a, b; Willemse et al., 1994). A single strain of FHV-1 was recently fully sequenced (Tai et al., 2010) as well as twenty four clinical isolates from Victoria, Australia and two vaccine strains from the USA (Vaz et al., 2016b). FHV-1 appears to have less intraspecies genomic sequence variability than some other alphaherpesviruses, such HSV-1, HSV-2, SuHV-1, and BHV-1 (Johnston et al., 2017; Kolb et al., 2015; Kolb et al., 2017; Newman et al., 2015; Pfaff et al., 2016; Szpara et al., 2014).

FHV-1 is a member of the *Varicellovirus* genus, with an approximately 135,800 bp genome, which is composed of unique long (UL) and unique short (US) sequences, flanked by inverted repeat regions known as terminal and inverted repeat long (TRL, IRL) and inverted and terminal repeat short (IRL, TRS), respectively (Tai et al., 2010). Herpesviruses have been shown to be highly recombinagenic (Loncoman et al., 2017; Norberg et al., 2004; Norberg et al., 2015; Norberg et al., 2007; Razzouk et al., 1996; Schynts et al., 2003; Sijmons et al., 2015; Vaz et al., 2016a), with a slight bias towards the inverted repeat regions

(Lee et al., 2015), however *Vaz et al* (Vaz et al., 2016b) reported that no recombination was detected in FHV-1 in their genomic analysis. It has also been demonstrated that different isolates of FHV-1 have variable virulence in vivo (Gaskell et al., 2007; Hamano et al., 2003) similar to what has been shown in *herpes simplex virus type 1* (HSV-1), *herpes simplex virus type 2* (HSV-2), *equine herpes virus type 1* (EHV-1), and *bovine herpesvirus type 1* (BHV-1) (Brandt and Grau, 1990; Kaashoek et al., 1998; Matsumura et al., 1996; Taha et al., 1989). The role of the host in determining the severity of infection is currently poorly understood, but likely involves aspects of innate and acquired immunity.

The primary objective of the current study was to utilize deep sequencing of the FHV-1 viral genome to more thoroughly evaluate strain variation in shelter-housed cats across the USA and to perform recombination and phylogenetic analysis using global isolate sequence data from previously sequenced isolates of FHV-1 available from Genbank (Tai et al., 2010; Vaz et al., 2016b).

2. Results and Discussion

2.1 Sequencing and genomic assembly

Twenty-six FHV-1 isolates were collected by participating shelters from 8 states across the USA (Figure 1). The 26 isolates were sequenced using a single lane of the Illumina MiSeq, and the number of sequencing reads for this study ranged from 978,704 (KANS 04) to 1,940,936 (S5727) (Table 1). The quantity of reads mapping to the reference strain following reference assembly ranged from 71,845 (CALI 11) to 775,198 (PHIL 04). The average mapped read length ranged from 272 (KANS 10 and KANS 08) to 281 (MILW 02). The average coverage across the genome ranged from 109x (CALI 11) to 1,023x (PHIL 04).

De novo assembly was also performed on a small subset of the genomes to determine if reference assembly results in a significant increase in genomic variability, which could affect downstream experiments. The results are summarized in Figure 2A, which shows the differences in single nucleotide polymorphisms (SNPs), insertions/deletions (INDELs), and genome coverage between the CALI 11 reference and *de novo* assemblies. Briefly, the reference and *de novo* assemblies were largely identical, with some small differences. The reference assembly of CALI 11 resulted in complete coverage of the genome, however a small number of SNPs and INDELs were detected in and near the TRL as compared to the *de novo* assembly, and the strain C-27 reference. The CALI 11 *de novo* assembly resulted in reduced coverage of the TRL, and parts of the IRS, TRS, as well as a small region of the US. Five INDELS were also detected near the low coverage area, which we believe are artifacts based on the low coverage. The authors of the study of Australian derived FHV-1 sequences also compared reference to *de novo* assemblies and found them to be identical (Vaz et al., 2016b). The small differences between reference and *de novo* assemblies in this study, specifically the slight SNP asymmetry in the reference assembly, and the small coverage loss from the *de novo* assembly compared to the results by *Vaz et al* (Vaz et al., 2016b) may be due to CLC-Bio Genomic Workbench (present study) algorithm constraints versus the Geneious package. Because the reference assemblies did not appear to introduce significant amounts of variability, while also resulting in higher coverage, the reference assemblies were used for subsequent analysis. Downstream genomic distance and phylogenetic analysis

combining genomes from the current study, as well as previously published genomes (Vaz et al., 2016b) was also deemed unlikely to be significantly affected.

While most of the reference assembled FHV-1 strains exhibited complete coverage, some had reduced coverage in the inverted repeat areas (Figure 2), akin to what has been reported for HSV-1 and 2 (Kolb et al., 2011; Kolb et al., 2015; Szpara et al., 2014). Areas of high G-C content in the reference strain corresponded with areas of lower coverage from the isolates sequenced for this study, consistent with Illumina sequencing of other herpesviruses (Kolb et al., 2015; Lee et al., 2015). A close examination of the genomes sequenced by *Vaz et al* (Vaz et al., 2016b), also showed reduced coverage of some of those genomes in the same areas (data not shown).

2.2 DNA polymorphism analysis

For the isolates sequenced in this study, we first wanted to identify and map SNPs (e.g. differences between the consensus genomes of each viral isolate) throughout the full genomic dataset to determine if there were regions enriched with SNPs or establish if the SNPs were generally evenly distributed (Figure 2B). Using DNAsp, we found that the SNPs were generally evenly distributed throughout the coding regions of the genome, with some enrichment in the large repeat regions as has been seen in HSV-1 and 2 (Kolb et al., 2015; Lee et al., 2015; Szpara et al., 2014). The highest number (12) of SNPs in one position correlated to an area of low coverage located in the ICP4 gene region towards the end of the TRS region and is likely an artifact due to lower sequence quality of some of the genomes. Eight SNPs in one position were detected towards the start of the IRS region. Three SNPs were also detected at approximately the 121,400bp position in the US region of the genome, which also corresponds to lower coverage in some of the genomes. The number of SNPs found within all isolates sequenced for this study was low compared to herpes simplex viruses, (Johnston et al., 2017; Kolb et al., 2011; Szpara et al., 2014).

All isolates sequenced as a part of this study were found to contain both synonymous and non-synonymous amino acid substitutions. The greatest number of synonymous substitutions in one strain was 69 (MILW 10). the lowest number of synonymous substitutions in one strain was 18 (S5727). The greatest number of non-synonymous substitutions in one strain was 16 (WASH 01 and WASH 03) and the lowest was 2 (MILW 02). The Australian isolates included in phylogenetic and recombinational analyses in this study have previously been analyzed for amino acid substitutions (Vaz et al., 2016b). The greatest number of unique non-synonymous amino acid substitutions in one gene for isolates sequenced for this study was 5, in UL36 (large tegument protein) (Table 2); the Australian isolates were also found to contain the most variation in this region with 7 unique changes (Vaz et al., 2016b). This is unsurprising as UL36 is one of the largest genes present in FHV-1. In contrast, many of the Australian isolates were found to contain variation in the UL13 (tegument serine/threonine protein kinase) and ICP4 (transcriptional regulator ICP4) regions; none of the USA-derived isolates sequenced for this study contained amino acid variation in these regions. We found the second highest number of unique non-synonymous amino acid substitutions in one gene for isolates sequenced for this study in UL55 (nuclear protein UL55); the Australian isolates had only one amino acid change detected in one

strain. Similarly, we found 4 unique non-synonymous amino acid substitutions in UL15 (DNA packaging terminase subunit 1) for isolates sequenced for this study; the Australian isolates did not contain any amino acid variation in this region. The low number of non-synonymous substitutions differs from what has been seen in the simplex viruses, but is generally similar to what has been observed in varicella zoster virus (VZV) (Kolb et al., 2015; Lee et al., 2015; Peters et al., 2006).

Several isolates sequenced as a part of this study were found to contain non-synonymous amino acid substitutions in the UL30 (DNA polymerase catalytic subunit) and UL23 (thymidine kinase) gene regions. Four isolates were found to have non-synonymous substitutions in UL30 (DNA polymerase catalytic subunit) (MILW 03, MILW 10, WASH 01 and WASH 03). Only one strain was found to have non-synonymous substitutions in UL23 (thymidine kinase) (SANJ 01).

Although some of the Australian isolates contained amino acid variation in UL30, none of them contained amino acid variation in UL23. None of the isolates contained amino acid variation in UL42 (DNA polymerase processivity subunit). Amino acid substitutions in these genes (UL23/30/42) are of clinical interest because they occur in regions which are targeted by commonly used antiviral medications (Filer et al., 1995; Thomasy and Maggs, 2016). Antiviral resistance of HSV-1 has been documented amongst immunocompromised individuals (Morfin and Thouvenot, 2003), but there are no such reports for FHV-1 in cats. Although it is possible SNPs in these genes (UL23/30/42) may confer resistance to antiviral medications, these changes appear to be uncommon in the viruses analyzed. The possible association of SNPs in the UL30 and UL23 genes with antiviral resistance will require further study and the development of a standard resistant laboratory strain for comparison.

2.3 Microsatellite and tandem repeat detection analysis

For the isolates sequenced in this study, we identified and mapped microsatellites and tandem repeats, two types of short sequence repeats (SSRs), throughout the genome to determine if there were regions enriched with SSRs, or establish if the SSRs were evenly distributed. Tandem repeats are defined as short DNA nucleotide stretches, which are repeated adjacent to each other. Microsatellites are a category of tandem repeat however they are longer and generally form di-, tri, tetra, penta-, and hexa-repeat structures. To prevent possible asymmetry in the analysis, the terminal repeats were excluded from the analysis. Only six microsatellites were found (Figure 2B); all of which were located in the IRS region, being 83% conserved across the isolates (Figure 3). This is in contrast to previous findings for HSV-2, where most microsatellites were found in the UL region and a lower degree of conservation was observed (Kolb et al., 2015).

Twenty-six tandem repeats were detected within isolates sequenced for this study (Figure 2B). Fifty percent of these were located in the UL region, being 92% conserved across isolates (Figure 3). Forty-six percent of the tandem repeats were located in the IRS region, with 67% conservation. Only 1 was detected in the US region and was found to be conserved across all isolates. This distribution of tandem repeats across the genome and degree of conservation is similar to previous findings for HSV-2 (Kolb et al., 2015).

Neither tandem repeats nor microsatellites were detected in the TRL or IRL regions, which may be due to the short length of these regions. Both microsatellites and tandem repeats have been used in the past to rapidly characterize isolates of related viruses (Burrel et al., 2013; Renault et al., 2014) and may be useful for FHV-1 research in the future.

2.4 Genomic distance analysis

A previous report analyzing multiple FHV-1 genomes showed that there was low genomic interstrain distance in isolates obtained in Australia and the vaccine strains, with a maximum genetic distance of 0.01% between strains (Vaz et al., 2016b). First, we sought to examine the overall mean genomic distance between only the American isolates, which was determined to be 0.035%. The greatest genomic distance between two American strains was 0.114% (PHIL 10, WASH 03), and the lowest genetic distance at 0% (multiple isolates). Pairwise gap deletion was used in the distance calculations, which could result in distance underestimation, however because of the low number of short sequence repeats, and sequencing gaps, it is unlikely to significantly bias the result. It is uncertain why there is higher overall distance among the American strains (0.035%) versus, the Australian derived isolates (0.01%), however this may be due to the greater geographical distribution of the American isolates, whereas the Australian strains were collected from the Melbourne, Victoria area, with 14 coming from the same shelter. When the analysis included all available isolates, including vaccine, Australian, and American strains, the overall genomic distance between isolates was 0.093%, with the greatest pairwise distance being 0.195% (3224/04 and 117/68, 85/68 and 729/83) and the lowest pairwise distance at 0% (multiple isolates). This degree of low genetic diversity of FHV-1 is similar to that of VZV (Peters et al., 2006; Zell et al., 2012), however it is unclear why these viruses display a lower degree of genetic diversity than some other varicelloviruses, such as BHV-1. It may be possible, that genomic G-C content could be a contributing factor in intraspecies genomic distance, with VZV and FHV-1 exhibiting low G-C content (both 45.8%) and intraspecies distance (0.136 and 0.093% respectively), while SuHV-1 and BHV-1 have much higher G-C contents (73.6% and 72.6% respectively) and intraspecies overall distance (1.65% and 0.81% respectively) (Kolb et al., 2017).

2.5 Phylogenetic and recombination analysis

Before characterizing the phylogeny of all available FHV-1 isolates, we first established the validity of assigning clades due to the low genetic distance. To determine this, the *p*-distance frequencies were graphed, and low and high distance populations were observed (Figure 4), validating clade assignment. Genetic distance cutoffs for establishing clades have been previously used in phylogenetic analyses of porcine circovirus type 2 (PCV2), H5N1 influenza, and the *Varicellovirus* genus (Kolb et al., 2017; Segales et al., 2008; Xiao et al., 2015). Similarly, the genetic distance cutoff for the FHV-1 clades (0.00058; Figure 5) was established by ascertaining the trough between the low and high distance populations and, was additionally aided by overlaying a kernel density plot. A maximum likelihood tree including *canine herpes virus type 1* (CHV-1) as an outgroup was generated, and suggested four FHV-1 clades, that primarily correlated with geographic location (Figure 5). Next, a phylogenetic network which can show phylogenetic dissonance within the dataset and may infer recombination was generated and recovered the main four clades (Figure 6A). With

only a few exceptions, the FHV-1 clades followed geographic lines, where clade 1 contained isolates from the USA, clade 2 was geographically mixed, and clade 3 and 4 contained only Australian isolates. In addition, the isolates from the USA were often clustered by geographic location (e.g. PHIL 01, PHIL 03, and PHIL 04; Figures 5 and 6), which may represent spread within the shelter environment. The genetic distances between the clades were also measured (Figure 6B), resulting in all values above the 0.00058 cutoff. The analysis found that the lowest distance (0.001066) was between the Australian clades 3 and 4, and highest distance (0.001434) was between clades 2 and 4. Six of the FHV-1 isolates (729/83, 221/71, FLOR 04, FLOR 05, MILW 03, and MILW 10) did not clearly sort into the four clades, which suggests that these strains may be interclade recombinants or representatives of additional clades.

Recombination in herpesviruses has been shown to be pervasive (Dohner et al., 1988; Henderson et al., 1990; Kolb et al., 2017; Loncoman et al., 2017; Norberg et al., 2004; Norberg et al., 2015; Norberg et al., 2007; Razzouk et al., 1996; Schynts et al., 2003; Sijmons et al., 2015; Vaz et al., 2016a), and so we next sought to investigate recombination in FHV-1. Prior work by *Vaz et al* (Vaz et al., 2016b) did not detect recombination, likely due to the low genetic variability of the Australian FHV-1 sequences. In the current study comprising the 53 available genomic sequences, reticulations within the phylogenetic network (Figure 6A) implied recombination within the dataset and, the pairwise homoplasty index (PHI) test for recombination found significant evidence of recombination (p = <0.0001). As mentioned above, there were six outlying strains, that did not clearly fit into one of the four clades, and may be interclade recombinants. To attempt to address this possibility, consensus sequences for each of the four clades was generated, and a new phylogenetic network produced (Figure 7A), along with the six outliers, similar to analyses conducted by *Norberg et al* with VZV (Norberg et al., 2015). The pattern of the network is consistent with both rapid population expansion, and recombination. The PHI recombination test resulted in statistically significant support for recombination (p = <0.0001). Bootscan phylogenetic analysis was also performed on the consensus sequences, and the six outliers and detected recombination signals between the different sequences (Figure 7A). Further RDP4 analysis (Figure 7B) identified contrasting phylogenetic elements, which implied a common recombination event in clades 2 and 3, along with the two outlying Milwaukee derived strains (MILW 03 and MILW 10), with a second recombination event in clade 3. The results suggest that the two outlying Milwaukee derived strains may indeed be interclade recombinants, however while the Bootscan analysis did detect some recombination signals in the remaining outliers, the results were largely inconclusive, likely due to low variability. While the consensus based phylogenetic network does suggest that the 729/83, FLOR 04, and FLOR 05 isolates may represent a separate clade however, this will require analysis with additional strains.

3. Materials and Methods

3.1 Cells

Crandell Rees feline kidney cells (CRFK) were used to generate viral stocks and were cultured in Dulbecco's modified Eagle's medium (DMEM) with 10% fetal bovine serum,

100 units/ml penicillin and 100 μg/ml streptomycin sulfate. For viral DNA isolation, the infections were carried out in DMEM with 2% fetal bovine serum, 100 units/ml penicillin, 100 μg/ml streptomycin sulfate and 250 μg/ml amphotericin B.

3.2 Viruses

All viruses included in this study are shown in Table 1. Publicly available sequences for 28 previously sequenced isolates were included in the recombination and phylogenetic analysis (Papageorgiou et al., 2016; Tai et al., 2010; Vaz et al., 2016b). Twenty-five additional FHV-1 viral isolates were sequenced for this study and were collected from cats in 8 geographically distinct locations in the USA (Figure 1). All procedures were performed in accordance with an approved University of Wisconsin-Madison Institutional Animal Care and Use Committee protocol. All of these cats were housed in animal shelters at the time of sampling. One oropharyngeal swab was taken from each cat by brushing the oropharyngeal area firmly for around 10 seconds. The swabs were then placed into a transport medium (Universal Viral Transport, Becton, Dickinson and Company), labeled and double bagged to prevent cross-contamination. Gloves were changed between animals. The swabs were shipped overnight to the UW-Madison Brandt laboratory for viral isolation. One isolate sequenced for this study (S5727) was obtained from another laboratory and had been collected as previously described (Nasisse et al., 1989).

3.3 Viral DNA preparation

Clinical samples were immediately refrigerated on receipt prior to viral isolation. A 1 ml aliquot of each sample was added to individual 100 mm tissue culture plates with maximally confluent Crandell Rees feline kidney cells (CRFK) along with 1 ml of Dulbecco's modified Eagle's medium containing 2% fetal bovine serum, 100 units/ml penicillin, 100 μg/ml streptomycin sulfate and 250 μg/ml amphotericin B (DMEM) before being incubated at 37°C for 60 minutes. An additional 4 ml of DMEM was then added to each plate before being incubated at 37°C and checked daily for 7 days until 100% cytopathic effect (CPE) was observed. The cells and media were scraped and pipetted from the plate and placed in a conical tube for centrifugation at 600 × g for 10 minutes at 4°C in a Sorvall X1R Legend centrifuge. The supernatant was removed, and the pellet was re-suspended in 750 μL of the reserved culture medium. The remainder of the culture supernatant was stored at 4°C. The re-suspended pellet was subjected to three freeze-thaw cycles and centrifuged at 600 × g for 10 minutes at 4°C (Sorvall X1R Legend centrifuge). The resultant supernatant was combined with the saved culture medium and stored in 200 μL aliquots at −80°C.

Viral DNA was prepared using a modification of a previously published protocol (36). Briefly, a thawed vial of virus stock was added to 12ml of DMEM in a 15 ml conical tube. Two ml of this mixture per plate was added to 6 confluent 100 mm tissue culture plates of CRFK cells and incubated at 37°C for 60 minutes. An additional 4 ml of DMEM was added to each plate before being incubated at 37°C and checked daily until 100% CPE was observed. The cells and media were scraped and added to a single 50 ml conical tube before being centrifuged at 600 × g for 10 minutes at 4°C (Sorvall Legend × 1R centrifuge). The supernatant was then stored at 4°C. The pellets were re-suspended in 5 ml of the saved supernatant and subjected to three freeze-thaw cycles. All supernatants were combined and

centrifuged at 600 × g for 10 minutes at 4°C. The resultant supernatant was then centrifuged at 600 × g for 5 minutes at 4°C. The supernatant was layered onto a 36% sucrose cushion in 0.1 M phosphate-buffered saline and centrifuged for 80 min at 24,000 × g at 4°C (Sorvall WX Ultra Series ultracentrifuge). The pellet was re-suspended in 1 ml of TE buffer per tube (10 mM Tris [pH 7.4], 1 mM EDTA) with 0.15 M sodium acetate and 50 μg/ml RNase A and then incubated for 15 min at 37°C. Proteinase K and SDS (50 μg/ml and 0.1%, final concentrations respectively) were added, and the solution was incubated for 15 min at 37°C. The viral DNA was purified by phenol-chloroform extraction and ethanol precipitation, incubated with 50 μg/ml RNase A for a further 15 minutes, re-suspended in deionized water, and stored at −20°C. DNA purity and concentration were analyzed using a Nanodrop Lite Spectrophotometer (Thermo Scientific).

3.5 Construction and sequencing of Illumina libraries

DNA was submitted to the University of Wisconsin-Madison Biotechnology Center for sequencing. DNA concentration was verified using the Qubit® dsDNA HS Assay Kit (Life Technologies, Grand Island, NY). Samples were prepared according the TruSeq Nano DNA LT Library Prep Kit (Illumina Inc., San Diego, California, USA) with minor modifications. Samples were sheared using a Covaris M220 Ultrasonicator (Covaris Inc, Woburn, MA, USA), and were size selected for an average insert size of 550 bp using SPRI bead based size exclusion. Quality and quantity of the finished libraries were assessed using an Agilent DNA1000 chip and Qubit® dsDNA HS Assay Kit, respectively. Libraries were standardized to 2μM. Paired end, 300 bp sequencing was performed using the Illumina MiSeq Sequencer and a MiSeq 600 bp (v3) sequencing cartridge. Images were analyzed using the standard Illumina Pipeline, version 1.8.2.

3.5 Genomic assembly and SNP/INDEL detection

For reference based assembly, paired-end sequencing reads were first trimmed (quality filtering not performed), and then aligned to the reference FHV-1 strain (C-27) using CLC-Bio Genomic Workbench (version 9.5.3). A consensus sequence was extracted from the aligned reads, all of which had a minimum threshold of 100× coverage. Gaps in the sequence were filled with “N’s”. Following genome annotation, the sequences were submitted to Genbank.

A small subset of genomes were also assembled using *de novo* assembly. For the *de novo* assembly, the trimmed paired-end reads were first aligned to the cat genome (GCF_000181335.3_Felis_catus_9.0) using CLC-Bio Genomic Workbench, and the unaligned reads were collected. The unaligned reads were used for *de novo* assembly, and the resulting contigs were aligned to the FHV-1 (C-27) genome. The genomic sequence was then extracted from the aligned contigs.

3.6 Genomic sequence alignments

Three genomic alignments were created: one assembly using only the sequences from samples collected as a part of the current study, a second alignment combining the sequences from the current study and the existing Genbank FHV-1 sequence data, and a final alignment comprising all of the available FHV-1 sequences, including those from the current study, and

canine herpesvirus type 1 (CHV-1; strain 0194) as an outgroup. All alignments were produced with MAFFT (ver 7) (Katoh and Standley, 2013).

3.7 DNA polymorphism, SNP/INDEL, and G-C content analysis

DNAsp (ver 5) (Librado and Rozas, 2009) was used to detect DNA polymorphisms across the sequences from samples collected as a part of this study. Alignment gaps were excluded with a sliding window of 100bp and a step size of 25 nucleotides. The overall interstrain genomic mean and pairwise distances were calculated using Mega 7 using the maximum composite likelihood model with pairwise deletion of gaps (Kumar et al., 2016). CLC-Bio Genomic Workbench (ver 9.5.3) was used to detect SNPs and INDELs compared to the FHV-1 reference strain (C-27).The G-C content of the reference FHV-1 strain (C-27) was assessed using Artemis (Carver et al., 2012).

3.8 Microsatellite and tandem repeat detection

Msatcommander (ver 0.8.2) (Faircloth, 2008; Rozen and Skaletsky, 2000) and Tandem Repeat Finder (ver 4.09) (Benson, 1999) were used to detect microsatellites and tandem repeats, respectively, in all sequences from isolates collected as a part of this study. Msatcommander was configured to detect mononucleotide to hexanucleotide repeats, with a mononucleotide length of 10, a dinucleotide repeat length of 6 and the remaining parameters using a repeat length of 4. Tandem Repeat Finder was set to detect tandem repeats with a match of 2, mismatch of 5, delta of 5, PM of 80, minimum score of 40 and maximum period of 500. Microsatellites which were detected by both Msatcommander and Tandem Repeat Finder were not removed. Tandem repeats and microsatellites were deemed conserved if the short sequence repeat (SSR) was detected in all of the isolates sequenced for the present study.

3.9 Phylogenetic and recombination analysis

The FHV-1 phylogenetic clade cutoff was determined by graphing the frequency of p-distances, which were calculated using MEGA 7. The *p*-distance frequency graph was generated using the R software package (version 3.4.1). A kernel density plot also generated in R to assist in determining the clade cutoff value by finding the trough between the low and high p-value populations. Initial phylogenetic analysis of the FHV-1 isolates, which included CHV-1 as an outgroup was performed by generating a maximum likelihood tree using RAxMLGUI (v. 1.5b1), (Berger et al., 2011) with the GTRGAMMA substitution model, and 500 replicate bootstraps. The phylogenetic network was generated using Splitstree (v4.14.4) (Huson and Bryant, 2006). Jmodeltest (ver 2.1.10) (Darriba et al., 2012; Guindon and Gascuel, 2003) was used to determine the nucleotide substitution optimal models for RAxML and Splitstree.

Recombination was assessed in all available FHV-1 isolates using several methods. First, the PHI (pairwise homoplasty index) (Bruen et al., 2006) statistical test for recombination was calculated was using Splitstree (ver 4.14.4). The second method was the creation of representative recombination Bootscan plots using RDP4 (ver Beta 4.91) with a sliding window of 1500 nucleotides, a step size of 750 bp, and the Jin and Nei substitution model. Possible recombination between FHV-1 clades was examined by generating a consensus

sequence for each of the clades, and generating a new phylogenetic network using Splitstree. Further recombination analysis was performed using the RDP, Bootscan, GENECONV, MaxChi, Chimera, and Siscan methods within RDP4.

3.10 Nucleotide sequence accession numbers

All isolates used for analysis in this study are shown in Table 1 and are available for viewing and download on the GenBank website (https://www.ncbi.nlm.nih.gov/genbank/). The alignments are available at (http://sites.ophth.wisc.edu/brandt/).

Acknowledgments

The authors thank the University of Wisconsin Biotechnology Center DNA Sequencing Facility for providing Illumina sequencing facilities and services. The authors would also like to thank Dr. Julie Andersen, Dr. Cooper Brookshire, Kristen Cooley CVT, Dr. Jen Dalmasso, Dr. Sarah Frei, Dr. McLean Gunderson, Dr. Libby Gutting, Dr. Hillary Herendeen, Dr. David Maggs, Jenni Rose McKay, Dr. Sharon Ostermann, Dr. Lauren Park, Dr. Emily Purvis, Dr. Christine Solis, Dr. Aleisha Swartz, Dr. Margaret Wixson, Dr. Kimberly Woodruff and Dr. Mark Verdino for their assistance in acquiring the samples sequenced in this study.

Funding

This project was supported by grants from the University of Wisconsin-Madison Companion Animal Fund; University of Wisconsin-Madison Shelter Program Maddie's Fund, Faculty start-up funds from the University of Wisconsin-Madison School of Veterinary Medicine (to GJM); an NIH Core Grant for Vision Research (P30EY016665) and the Clinical and Translational Science Award (CTSA) program, through the NIH National Center for Advancing Translational Sciences (NCATS), grant (UL1TR000427). Additional support was provided by an unrestricted grant to the Department of Ophthalmology and Visual Sciences from Research to Prevent Blindness, Inc. The content is solely the responsibility of the authors and does not necessarily represent the official views of the NIH or other funding bodies.

References

Benson G. Tandem repeats finder: a program to analyze DNA sequences. Nucleic Acids Res. 1999; 27:573–580. [PubMed: 9862982]

Berger SA, Krompass D, Stamatakis A. Performance, accuracy, and Web server for evolutionary placement of short sequence reads under maximum likelihood. Syst Biol. 2011; 60:291–302. [PubMed: 21436105]

Brandt CR, Grau DR. Mixed infection with herpes simplex virus type 1 generates recombinants with increased ocular and neurovirulence. Invest Ophthalmol Vis Sci. 1990; 31:2214–2223. [PubMed: 2173682]

Bruen TC, Philippe H, Bryant D. A simple and robust statistical test for detecting the presence of recombination. Genetics. 2006; 172:2665–2681. [PubMed: 16489234]

Burrel S, Ait-Arkoub Z, Voujon D, Deback C, Abrao EP, Agut H, Boutolleau D. Molecular characterization of herpes simplex virus 2 strains by analysis of microsatellite polymorphism. J Clin Microbiol. 2013; 51:3616–3623. [PubMed: 23966512]

Carver T, Harris S, Berriman M, Parkhill J, McQuillan J. Artemis: an integrated platform for visualization and analysis of high-throughput sequence-based experimental data. Bioinformatics. 2012; 28:464–469. [PubMed: 22199388]

Darriba D, Taboada GL, Doallo R, Posada D. jModelTest 2: more models, new heuristics and parallel computing. Nat Methods. 2012; 9:772.

Dohner DE, Adams SG, Gelb LD. Recombination in tissue culture between varicella-zoster virus strains. J Med Virol. 1988; 24:329–341. [PubMed: 2835429]

Faircloth BC. msatcommander: detection of microsatellite repeat arrays and automated, locus-specific primer design. Mol Ecol Resour. 2008; 8:92–94. [PubMed: 21585724]

Filer CW, Ramji JV, Allen GD, Brown TA, Fowles SE, Hollis FJ, Mort EE. Metabolic and pharmacokinetic studies following oral administration of famciclovir to the rat and dog. Xenobiotica. 1995; 25:477–490. [PubMed: 7571721]

Gaskell R, Dawson S, Radford A, Thiry E. Feline herpesvirus. Veterinary research. 2007; 38:337–354. [PubMed: 17296160]

Gaskell R, Willoughby K. Herpesviruses of carnivores. Vet Microbiol. 1999; 69:73–88. [PubMed: 10515274]

Gaskell RM, Povey RC. Experimental induction of feline viral rhinotracheitis virus re-excretion in FVR-recovered cats. Vet Rec. 1977; 100:128–133. [PubMed: 191978]

Gould D. Feline herpesvirus-1: ocular manifestations, diagnosis and treatment options. J Feline Med Surg. 2011; 13:333–346. [PubMed: 21515221]

Guindon S, Gascuel O. A simple, fast, and accurate algorithm to estimate large phylogenies by maximum likelihood. Syst Biol. 2003; 52:696–704. [PubMed: 14530136]

Hamano M, Maeda K, Kai K, Mochizuki M, Tohya Y, Akashi H. A novel genetic marker to differentiate feline herpesvirus type 1 field isolates. Veterinary microbiology. 2005; 106:195–200. [PubMed: 15778025]

Hamano M, Maeda K, Mizukoshi F, Mochizuki M, Tohya Y, Akashi H, Kai K. Genetic rearrangements in the gC gene of the feline herpesvirus type 1. Virus genes. 2004; 28:55–60. [PubMed: 14739651]

Hamano M, Maeda K, Mizukoshi F, Une Y, Mochizuki M, Tohya Y, Akashi H, Kai K. Experimental infection of recent field isolates of feline herpesvirus type 1. J Vet Med Sci. 2003; 65:939–943. [PubMed: 12951431]

Hara M, Fukuyama M, Suzuki Y, Kisikawa S, Ikeda T, Kiuchi A, Tabuchi K. Detection of feline herpesvirus 1 DNA by the nested polymerase chain reaction. Veterinary microbiology. 1996; 48:345–352. [PubMed: 9054130]

Hartley C. Aetiology of corneal ulcers assume FHV-1 unless proven otherwise. J Feline Med Surg. 2010; 12:24–35. [PubMed: 20123484]

Henderson LM, Katz JB, Erickson GA, Mayfield JE. In vivo and in vitro genetic recombination between conventional and gene-deleted vaccine strains of pseudorabies virus. Am J Vet Res. 1990; 51:1656–1662. [PubMed: 2173449]

Herrmann SC, Gaskell RM, Ehlers B, Ludwig H. Characterization of the feline herpesvirus genome and molecular epidemiology of isolates from natural outbreaks and latent infections. Latent Herpes Virus Infections in Veterinary Medicine. 1984:321–336.

Huson DH, Bryant D. Application of phylogenetic networks in evolutionary studies. Mol Biol Evol. 2006; 23:254–267. [PubMed: 16221896]

Johnston C, Magaret A, Roychoudhury P, Greninger AL, Reeves D, Schiffer J, Jerome KR, Sather C, Diem K, Lingappa JR, Celum C, Koelle DM, Wald A. Dual-strain genital herpes simplex virus type 2 (HSV-2) infection in the US, Peru, and 8 countries in sub-Saharan Africa: A nested cross-sectional viral genotyping study. PLoS Med. 2017; 14:e1002475. [PubMed: 29281620]

Kaashoek MJ, Rijsewijk FA, Ruuls RC, Keil GM, Thiry E, Pastoret PP, Van Oirschot JT. Virulence, immunogenicity and reactivation of bovine herpesvirus 1 mutants with a deletion in the gC, gG, gI, gE, or in both the gI and gE gene. Vaccine. 1998; 16:802–809. [PubMed: 9627937]

Katoh K, Standley DM. MAFFT multiple sequence alignment software version 7: improvements in performance and usability. Mol Biol Evol. 2013; 30:772–780. [PubMed: 23329690]

Kawaguchi Y, Maeda K, Miyazawa T, Ono M, Kai C, Mikami T. Nucleotide sequence and characterization of the feline herpesvirus type 1 immediate early gene. Virology. 1994; 204:430–435. [PubMed: 8091674]

Kolb AW, Adams M, Cabot EL, Craven M, Brandt CR. Multiplex sequencing of seven ocular Herpes simplex virus Type-1 genomes: Phylogeny, sequence variability and SNP distribution. Invest Ophthalmol Vis Sci. 2011; 52:9061–9073. [PubMed: 22016062]

Kolb AW, Larsen IV, Cuellar JA, Brandt CR. Genomic, phylogenetic, and recombinant characterization of Herpes simplex virus Type 2 strains. J Virol. 2015; 89:6427–6434. [PubMed: 25855744]

Kolb AW, Lewin AC, Moeller Trane R, McLellan GJ, Brandt CR. Phylogenetic and recombination analysis of the herpesvirus genus varicellovirus. BMC Genomics. 2017; 18:887. [PubMed: 29157201]

Kumar S, Stecher G, Tamura K. MEGA7: Molecular Evolutionary Genetics Analysis version 7.0 for bigger datasets. Molecular biology and evolution. 2016:msw054.

Lee K, Kolb AW, Sverchkov Y, Cuellar JA, Craven M, Brandt CR. Recombination analysis of herpes simplex virus type 1 reveals a bias towards GC content and the inverted repeat regions. J Virol. 2015; 89:7214–7223. [PubMed: 25926637]

Librado P, Rozas J. DnaSP v5: a software for comprehensive analysis of DNA polymorphism data. Bioinformatics. 2009; 25:1451–1452. [PubMed: 19346325]

Loncoman CA, Vaz PK, Coppo MJ, Hartley CA, Morera FJ, Browning GF, Devlin JM. Natural recombination in alphaherpesviruses: Insights into viral evolution through full genome sequencing and sequence analysis. Infect Genet Evol. 2017; 49:174–185. [PubMed: 28017915]

Maeda K, Horimoto T, Norimine J, Kawaguchi Y, Tomonaga K, Niikura M, Kai C, Takahashi E, Mikami T. Identification and nucleotide sequence of a gene in feline herpesvirus type 1 homologous to the herpes simplex virus gene encoding the glycoprotein B. Archives of virology. 1992; 127:387–397. [PubMed: 1333759]

Maeda K, Kawaguchi Y, Kamiya N, Ono M, Tohya Y, Kai C, Mikami T. Identification and nucleotide sequence of a gene in feline herpesvirus type 1 homologous to the herpes simplex virus gene encoding the glycoprotein H. Archives of virology. 1993; 132:183–191. [PubMed: 8394688]

Maeda K, Kawaguchi Y, Ono M, Tajima T, Mikami T. Comparisons among feline herpesvirus type 1 isolates by immunoblot analysis. Journal of Veterinary Medical Science. 1995a; 57:147–150. [PubMed: 7756409]

Maeda K, Kawaguchi Y, Ono M, Tajima T, Mikami T. Restriction endonuclease analysis of field isolates of feline herpesvirus type 1 and identification of heterogeneous regions. Journal of clinical microbiology. 1995b; 33:217–221. [PubMed: 7699046]

Maggs DJ, Clarke HE. Relative sensitivity of polymerase chain reaction assays used for detection of feline herpesvirus type 1 DNA in clinical samples and commercial vaccines. American journal of veterinary research. 2005; 66:1550–1555. [PubMed: 16261828]

Matsumura T, O'Callaghan DJ, Kondo T, Kamada M. Lack of virulence of the murine fibroblast adapted strain, Kentucky A (KyA), of equine herpesvirus type 1 (EHV-1) in young horses. Vet Microbiol. 1996; 48:353–365. [PubMed: 9054131]

Morfin F, Thouvenot D. Herpes simplex virus resistance to antiviral drugs. J Clin Virol. 2003; 26:29–37. [PubMed: 12589832]

Nasisse MP, Guy JS, Davidson MG, Sussman WA, Fairley NM. Experimental ocular herpesvirus infection in the cat. Sites of virus replication, clinical features and effects of corticosteroid administration. Invest Ophthalmol Vis Sci. 1989; 30:1758–1768. [PubMed: 2474518]

Newman RM, Lamers SL, Weiner B, Ray SC, Colgrove RC, Diaz F, Jing L, Wang K, Saif S, Young S, Henn M, Laeyendecker O, Tobian AA, Cohen JI, Koelle DM, Quinn TC, Knipe DM. Genome Sequencing and Analysis of Geographically Diverse Clinical Isolates of Herpes Simplex Virus 2. J Virol. 2015; 89:8219–8232. [PubMed: 26018166]

Norberg P, Bergstrom T, Rekabdar E, Lindh M, Lijeqvist J. Phylogenetic analysis of clinical herpes simplex virus type 1 isolates identified three genetic groups and recombinant viruses. J Virol. 2004; 78:10755–10764. [PubMed: 15367642]

Norberg P, Depledge DP, Kundu S, Atkinson C, Brown J, Haque T, Hussaini Y, MacMahon E, Molyneaux P, Papaevangelou V, Sengupta N, Koay ES, Tang JW, Underhill GS, Grahn A, Studahl M, Breuer J, Bergstrom T. Recombination of globally circulating varicella-zoster virus. J Virol. 2015; 89:7133–7146. [PubMed: 25926648]

Norberg P, Kasubi MJ, Haarr L, Bergstrom T, Liljeqvist JA. Divergence and recombination of clinical herpes simplex virus type 2 isolates. J Virol. 2007; 81:13158–13167. [PubMed: 17881457]

Papageorgiou KV, Suarez NM, Wilkie GS, McDonald M, Graham EM, Davison AJ. Genome sequence of canine herpesvirus. PLoS One. 2016; 11:e0156015. [PubMed: 27213534]

Peters GA, Tyler SD, Grose C, Severini A, Gray MJ, Upton C, Tipples GA. A full-genome phylogenetic analysis of varicella-zoster virus reveals a novel origin of replication-based genotyping scheme and evidence of recombination between major circulating clades. J Virol. 2006; 80:9850–9860. [PubMed: 16973589]

Pfaff F, Groth M, Sauerbrei A, Zell R. Genotyping of herpes simplex virus type 1 by whole-genome sequencing. J Gen Virol. 2016; 97:2732–2741. [PubMed: 27558891]

Razzouk BI, Srinivas S, Sample CE, Singh V, Sixbey JW. Epstein-Barr Virus DNA recombination and loss in sporadic Burkitt's lymphoma. J Infect Dis. 1996; 173:529–535. [PubMed: 8627013]

Reagan KL, Hawley JR, Lappin MR. Concurrent administration of an intranasal vaccine containing feline herpesvirus-1 (FHV-1) with a parenteral vaccine containing FHV-1 is superior to parenteral vaccination alone in an acute FHV-1 challenge model. Vet J. 2014; 201:202–206. [PubMed: 24873978]

Renault T, Tchaleu G, Faury N, Moreau P, Segarra A, Barbosa-Solomieu V, Lapègue S. Genotyping of a microsatellite locus to differentiate clinical Ostreid herpesvirus 1 specimens. Vet Res. 2014; 45:3. [PubMed: 24410800]

Rozen S, Skaletsky H. Primer3 on the WWW for general users and for biologist programmers. Methods Mol Biol. 2000; 132:365–386. [PubMed: 10547847]

Schynts F, Meurens F, Detry B, Vanderplasschen A, Thiry E. Rise and survival of bovine herpesvirus 1 recombinants after primary infection and reactivation from latency. J Virol. 2003; 77:12535–12542. [PubMed: 14610176]

Segales J, Olvera A, Grau-Roma L, Charreyre C, Nauwynck H, Larsen L, Dupont K, McCullough K, Ellis J, Krakowka S, Mankertz A, Fredholm M, Fossum C, Timmusk S, Stockhofe-Zurwieden N, Beattie V, Armstrong D, Grassland B, Baekbo P, Allan G. PCV-2 genotype definition and nomenclature. Vet Rec. 2008; 162:867–868. [PubMed: 18587066]

Sijmons S, Thys K, Mbong Ngwese M, Van Damme E, Dvorak J, Van Loock M, Li G, Tachezy R, Busson L, Aerssens J, Van Ranst M, Maes P. High-throughput analysis of human cytomegalovirus genome diversity highlights the widespread occurrence of gene-disrupting mutations and pervasive recombination. J Virol. 2015

Szpara ML, Gatherer D, Ochoa A, Greenbaum B, Dolan A, Bowden RJ, Enquist LW, Legendre M, Davison AJ. Evolution and diversity in human herpes simplex virus genomes. J Virol. 2014; 88:1209–1227. [PubMed: 24227835]

Taha MY, Clements GB, Brown SM. The herpes simplex virus type 2 (HG52) variant JH2604 has a 1488 bp deletion which eliminates neurovirulence in mice. J Gen Virol. 1989; 70(Pt 11):3073–3078. [PubMed: 2555437]

Tai SH, Niikura M, Cheng HH, Kruger JM, Wise AG, Maes RK. Complete genomic sequence and an infectious BAC clone of feline herpesvirus-1 (FHV-1). Virology. 2010; 401:215–227. [PubMed: 20304455]

Thiry E, Addie D, Belák S, Boucraut-Baralon C, Egberink H, Frymus T, Gruffydd-Jones T, Hartmann K, Hosie MJ, Lloret A, Lutz H, Marsilio F, Pennisi MG, Radford AD, Truyen U, Horzinek MC. Feline herpesvirus infection. ABCD guidelines on prevention and management. J Feline Med Surg. 2009; 11:547–555. [PubMed: 19481034]

Thomasy SM, Maggs DJ. A review of antiviral drugs and other compounds with activity against feline herpesvirus type 1. Vet Ophthalmol. 2016; 19(Suppl 1):119–130. [PubMed: 27091747]

Vaz PK, Horsington J, Hartley CA, Browning GF, Ficorilli NP, Studdert MJ, Gilkerson JR, Devlin JM. Evidence of widespread natural recombination among field isolates of equine herpesvirus 4 but not among field isolates of equine herpesvirus 1. J Gen Virol. 2016a; 97:747–755. [PubMed: 26691326]

Vaz PK, Job N, Horsington J, Ficorilli N, Studdert MJ, Hartley CA, Gilkerson JR, Browning GF, Devlin JM. Low genetic diversity among historical and contemporary clinical isolates of felid herpesvirus 1. BMC Genomics. 2016b; 17:704. [PubMed: 27589862]

Willemse MJ, Chalmers WSK, Cronenberg AM, Pfundt R, Strijdveen IG, Sondermeijer PJ. The gene downstream of the gC homologue in feline herpesvirus type 1 is involved in the expression of virulence. Journal of general virology. 1994; 75:3107–3116. [PubMed: 7964620]

Xiao CT, Halbur PG, Opriessnig T. Global molecular genetic analysis of porcine circovirus type 2 (PCV2) sequences confirms the presence of four main PCV2 genotypes and reveals a rapid increase of PCV2d. J Gen Virol. 2015; 96:1830–1841. [PubMed: 25711965]

Zell R, Taudien S, Pfaff F, Wutzler P, Platzer M, Sauerbrei A. Sequencing of 21 varicella-zoster virus genomes reveals two novel genotypes and evidence of recombination. J Virol. 2012; 86:1608–1622. [PubMed: 22130537]

Highlights

- Twenty-six FHV-1 isolates were collected from 8 distinct locations across the USA and sequenced.
- The overall genomic interstrain genetic distance between all available global isolates was 0.093%.
- Phylogenetic analysis found evidence of four main clades.
- Recombination analysis suggested interclade recombination has occurred.

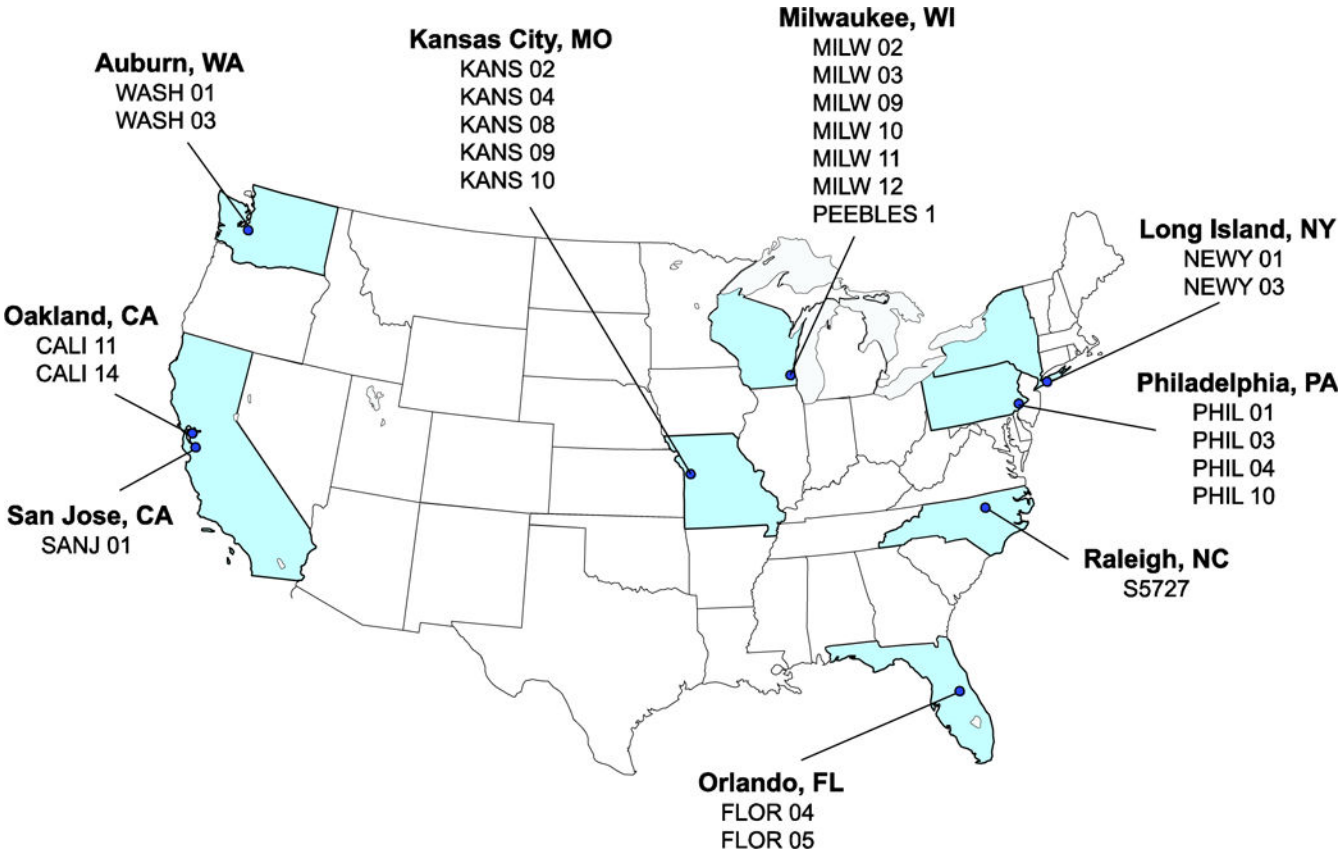

Figure 1.

Sources of viral isolates. The geographic locations and the specific isolates in the USA from which FHV-1 isolates were collected and sequenced are shown.

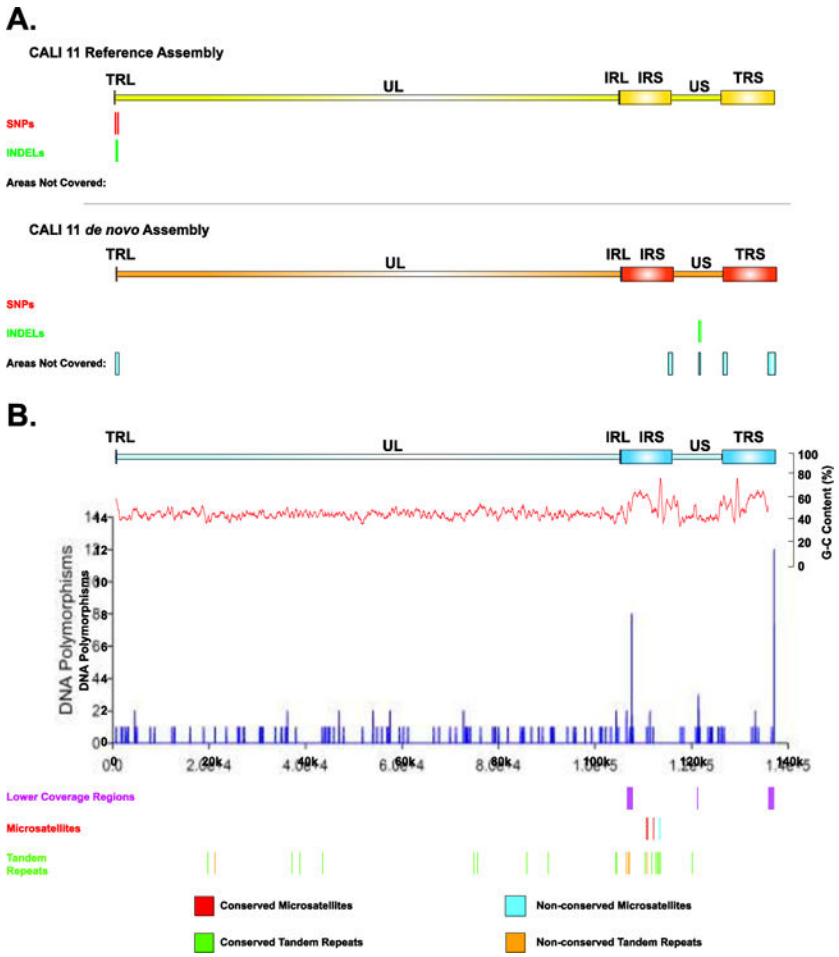

Figure 2.

Genome assembly method comparison and structural analysis. Panel A shows the comparison of reference versus *de novo* assembly SNP/INDELS and coverage. A diagram showing the difference between reference and *de novo* assembly of the CALI 11 isolate. SNPs and INDELS particular to each assembly method are shown below the genome diagrams respectively. The areas of the de novo assembly not covered are shown in blue, at the bottom of the figure. Panel B depicts the structural analysis of the FHV-1 genome. A schematic diagram of the FHV-1 genome is shown at the top of the figure. G-C content of the reference strain (C-27) is shown in red, immediately below the schematic. DNA polymorphisms in all isolates sequenced for this study are shown in dark blue in the graph. Areas of low coverage are shown directly below the DNA polymorphisms in purple. The positions of conserved and non-conserved microsatellites from all isolates sequenced for this study are shown in red and light blue, respectively. The positions of conserved and non-conserved tandem repeats from all isolates sequenced for this study are shown in green and orange, respectively.

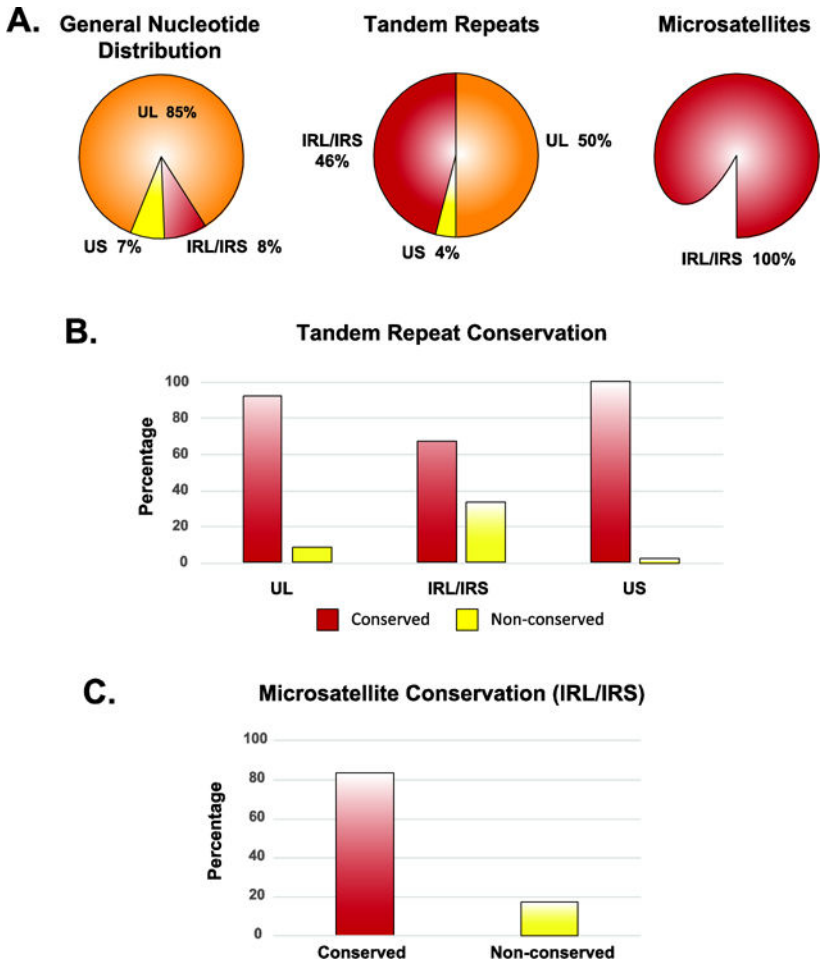

Figure 3.

Localization of microsatellites and tandem repeats. In panel A, the left pie chart shows the general distribution of genomic nucleotides in each of FHV-1 genomic regions, the center chart shows the genomic distribution of tandem repeats, and the distribution of microsatellites. Panel B shows the relative tandem repeat conservation in the UL, IRL/IRS, and US regions. Panel C shows microsatellite conservation in the IRL/IRS region.

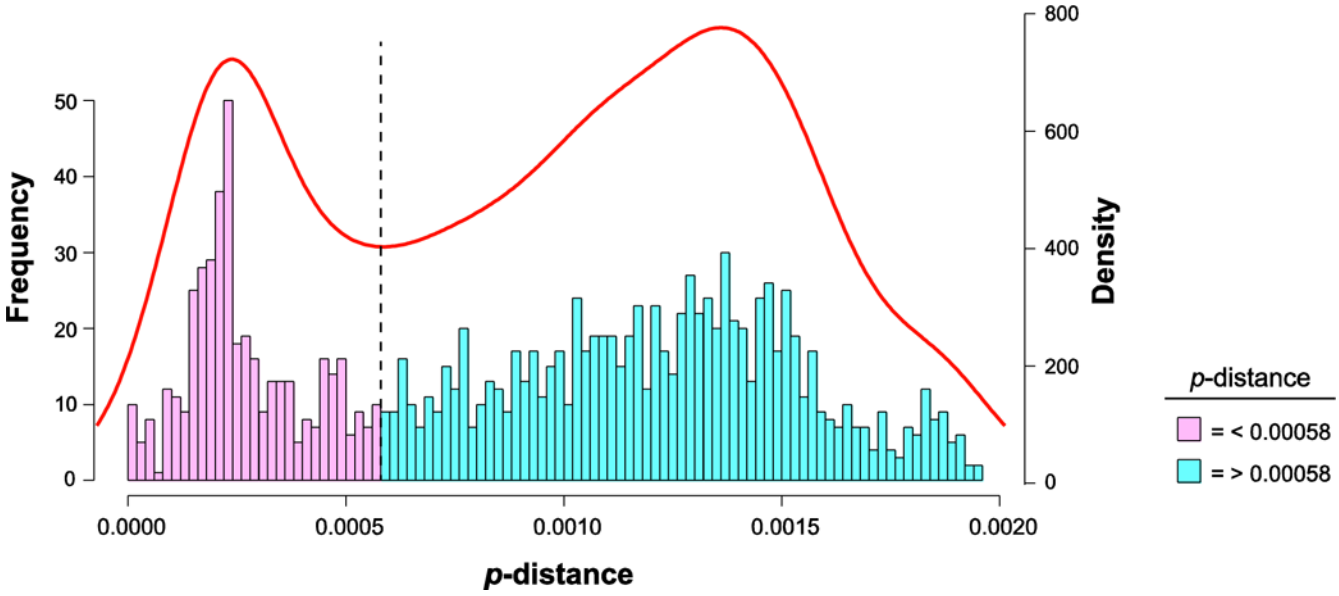

Figure 4.

Histogram establishing a FHV-1 clade cutoff. The pairwise distances were calculated between each of the 53 FHV-1 sequences, and the frequency of the distances was plotted in a histogram. A kernel density plot (red line) was superimposed onto the histogram to aid in finding the trough between the low and high *p*-distance populations. The vertical dotted line represents the clade cutoff value (0.00058). Frequency bins above 0.00058 were colored cyan, and below 0.00058 were colored pink.

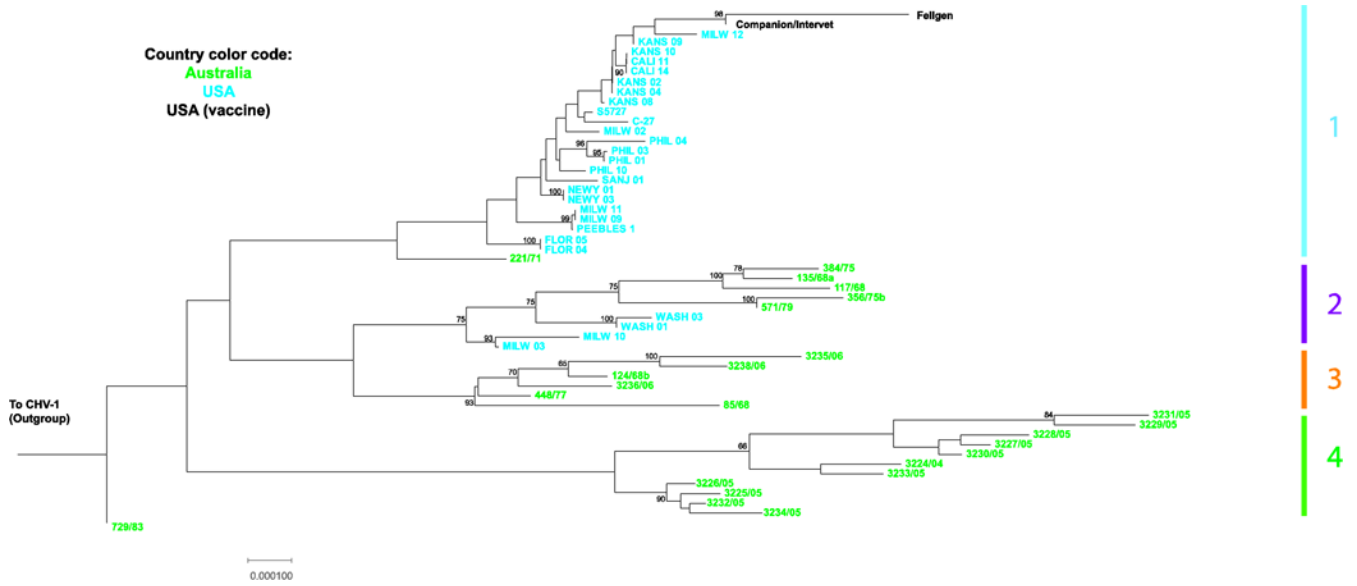

Figure 5.

Maximum likelihood tree of all isolates of FHV-1 with a CHV-1 outgroup, showing details of the FHV-1 node. Isolates of FHV-1 isolated in the USA are shown in blue, vaccine isolates from the USA are shown in black and isolates isolated in Australia are shown in red. The canine outgroup (CHV/0194) is shown in green. FHV-1 clades 1, 2, 3 and 4 are delineated on the right of the diagram. The tree is drawn to scale, with branch lengths measured in the number of substitutions per site. Bootstrap values over 60% are shown next to the associated branch. Created using GTR+Gamma model and 500 iterations with RAxML (ver 1.5b1).

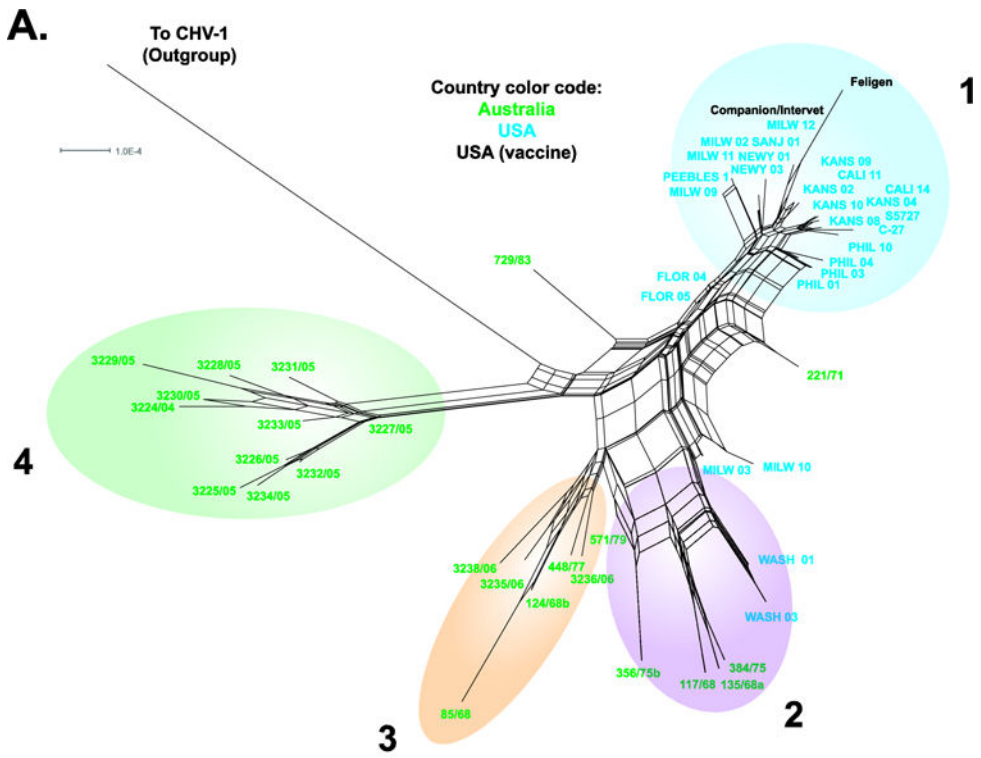

B.

Between Clade Mean Distances

	1	2	3
1			
2	0.001090		
3	0.001352	0.001146	
4	0.001432	0.001434	0.001066

Figure 6.

Phylogenetic network including all available sequences of FHV-1 with a CHV-1 outgroup. Splitstree was used to generate the network, and the Kimura 2-parameter substitution model was used with a *p*-inverse value of 0 and a shape value of 0.761 based on nucleotide substitution modeling using Jmodeltest2 (Panel A). Isolates of FHV-1 from the USA (including vaccine isolates) are shown in blue, isolates from Australia are shown in green, and the vaccine strains are shown in black. Four clades are shown; clade 1 (blue) includes USA isolates only, clade 2 (purple) includes Australian and USA isolates, clade 3 (orange) includes Australian isolates, and clade 4 (green) contains only Australian isolates. Panel B shows interclade genomic distance values.

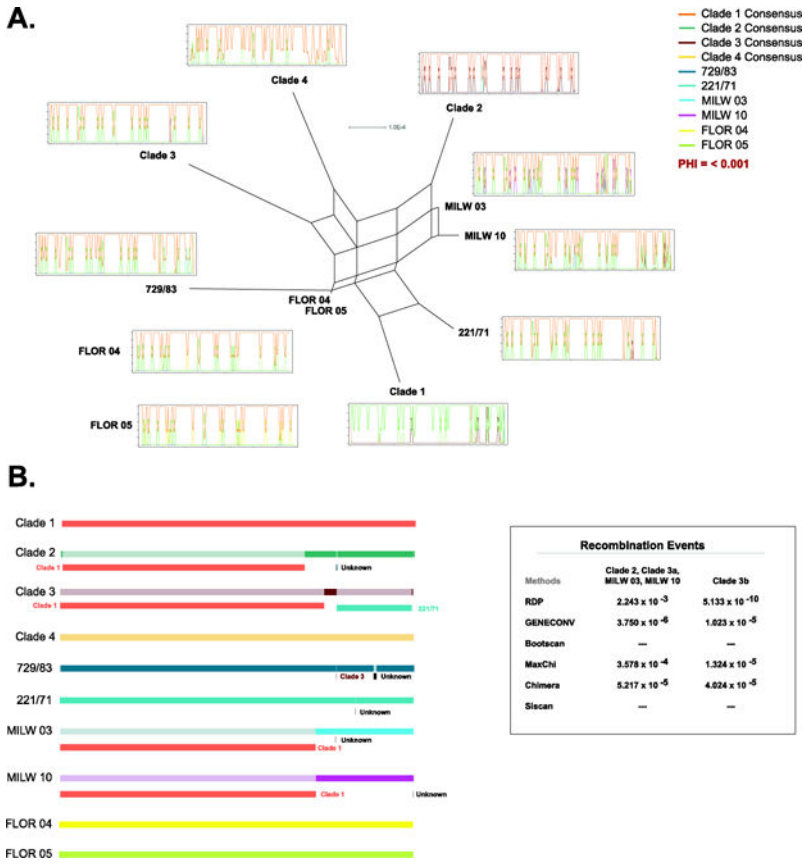

Figure 7.

Analysis of interclade recombination. To examine interclade recombination, a genomic consensus sequence was generated for each of the four main FHV-1 clades. A phylogenetic network (Panel A) comprising the four clades along with 6 outlying sequences (729/83, 221/71, FLOR_04, FLOR_05, MILW_03, and MILW_10) was generated using Splitstree (nucleotide substitution parameters were determined using Jmodeltest 2; K2P model, gamma = 0.05). Bootscans for each sequence were generated, and the line color key for each bootscan is shown in the upper right. Panel B shows the results of the RPD4 recombination analysis. Each consensus, and outlier sequence is represented by a colored bar, with contrasting phylogenetic segments shown directly below each represented genome. Unknown elements did not directly match any of the analyzed squences. One common recombination event was detected in clades 2, 3, MILW_03, and MILW_10, and a separate second event in clade 3. The statistical support for the RDP4 methods RDP, GENECONV, Bootscan, MaxChi, Chimera, and Siscan are shown to the right.

Table 1

A list of all viruses used for recombination and phylogenetic analysis showing country of origin.

Virus	Strain	Host	Country of Origin	GenBank accession number	Reference	Number Reads	Number of Reads Mapped to Reference Strain	Average Mapped Read Length (bp)	Average Coverage
FHV-1	C-27	Feline	USA	NC_013590.2/FJ478159.2	(Tai et al., 2010)				
FHV-1	FeligenRCP Virbac	Feline	USA	KR296657.1	(Vaz et al., 2016b)				
FHV-1	Companion Intervet Vaccine	Feline	USA	KR381803.1	(Vaz et al., 2016b)				
FHV-1	3227/05	Feline	Australia	KR381802.1	(Vaz et al., 2016b)				
FHV-1	3225/05	Feline	Australia	KR381801.1	(Vaz et al., 2016b)				
FHV-1	3234/05	Feline	Australia	KR381800.1	(Vaz et al., 2016b)				
FHV-1	3233/05	Feline	Australia	KR381799.1	(Vaz et al., 2016b)				
FHV-1	3232/05	Feline	Australia	KR381798.1	(Vaz et al., 2016b)				
FHV-1	3231/05	Feline	Australia	KR381797.1	(Vaz et al., 2016b)				
FHV-1	3230/05	Feline	Australia	KR381796.1	(Vaz et al., 2016b)				
FHV-1	3229/05	Feline	Australia	KR381795.1	(Vaz et al., 2016b)				
FHV-1	3228/05	Feline	Australia	KR381794.1	(Vaz et al., 2016b)				
FHV-1	3226/05	Feline	Australia	KR381793.1	(Vaz et al., 2016b)				
FHV-1	3224/04	Feline	Australia	KR381792.1	(Vaz et al., 2016b)				
FHV-1	3236/06	Feline	Australia	KR381791.1	(Vaz et al., 2016b)				
FHV-1	3238/06	Feline	Australia	KR381790.1	(Vaz et al., 2016b)				
FHV-1	3235/06	Feline	Australia	KR381789.1	(Vaz et al., 2016b)				
FHV-1	124/68b	Feline	Australia	KR381788.1	(Vaz et al., 2016b)				
FHV-1	85/68	Feline	Australia	KR381787.1	(Vaz et al., 2016b)				
FHV-1	135/68a	Feline	Australia	KR381786.1	(Vaz et al., 2016b)				
FHV-1	571/79	Feline	Australia	KR381785.1	(Vaz et al., 2016b)				
FHV-1	356/75b	Feline	Australia	KR381784.1	(Vaz et al., 2016b)				
FHV-1	448/77	Feline	Australia	KR381783.1	(Vaz et al., 2016b)				

Virus	Strain	Host	Country of Origin	GenBank accession number	Reference	Number Reads	Number of Reads Mapped to Reference Strain	Average Mapped Read Length (bp)	Average Coverage
FHV-1	384/75	Feline	Australia	KR381782.1	(Vaz et al., 2016b)				
FHV-1	221/71	Feline	Australia	KR381781.1	(Vaz et al., 2016b)				
FHV-1	117/68	Feline	Australia	KR381780.1	(Vaz et al., 2016b)				
FHV-1	729/83	Feline	Australia	KR381779.1	(Vaz et al., 2016b)				
FHV-1	CALI 11	Feline	USA	MH070326	Present Paper	1546382	71845	274	109×
FHV-1	CALI 14	Feline	USA	MH070339	Present Paper	1566852	79872	274	112×
FHV-1	FLOR 04	Feline	USA	MH070341	Present Paper	1191244	298425	276	461×
FHV-1	FLOR 05	Feline	USA	MH070327	Present Paper	1210088	363421	277	532×
FHV-1	KANS 02	Feline	USA	MH070348	Present Paper	1213966	685253	277	894×
FHV-1	KANS 04	Feline	USA	MH070337	Present Paper	978704	432069	275	697×
FHV-1	KANS 08	Feline	USA	MH070325	Present Paper	1169798	343164	272	558×
FHV-1	KANS 09	Feline	USA	MH070329	Present Paper	1055576	185677	275	283×
FHV-1	KANS 10	Feline	USA	MH070331	Present Paper	1008410	202371	272	337×
FHV-1	MILW 02	Feline	USA	MH070342	Present Paper	1287278	350784	281	509×
FHV-1	MILW 03	Feline	USA	MH070335	Present Paper	1118222	375265	276	601×
FHV-1	MILW 09	Feline	USA	MH070346	Present Paper	1081042	398696	276	589×
FHV-1	MILW 10	Feline	USA	MH070332	Present Paper	1123438	301374	275	466×
FHV-1	MILW 11	Feline	USA	MH070347	Present Paper	1544152	555960	274	827×
FHV-1	MILW 12	Feline	USA	MH070338	Present Paper	1136472	465781	277	701×
FHV-1	NEWY 01	Feline	USA	MH070324	Present Paper	1382250	336834	274	518×
FHV-1	NEWY 03	Feline	USA	MH070343	Present Paper	1023022	413453	274	639×
FHV-1	PEEBLES 1	Feline	USA	MH070340	Present Paper	1238784	189821	278	262×
FHV-1	PHIL 01	Feline	USA	MH070336	Present Paper	1089944	618907	278	822×
FHV-1	PHIL 03	Feline	USA	MH070334	Present Paper	1353794	314992	274	491×
FHV-1	PHIL 04	Feline	USA	MH070333	Present Paper	1281668	775198	278	1023×
FHV-1	PHIL 10	Feline	USA	MH070344	Present Paper	1284878	391677	276	578×
FHV-1	S5727	Feline	USA	MH070323	Present Paper	1940936	474304	274	671×

Virology. Author manuscript; available in PMC 2019 May 01.

Virus	Strain	Host	Country of Origin	GenBank accession number	Reference	Number Reads	Number of Reads Mapped to Reference Strain	Average Mapped Read Length (bp)	Average Coverage
FHV-1	SANJ 01	Feline	USA	MH070330	Present Paper	1240278	139896	278	208×
FHV-1	WASH 01	Feline	USA	MH070328	Present Paper	1461288	357555	278	533×
FHV-1	WASH 03	Feline	USA	MH070345	Present Paper	1510186	145571	274	210×
CHV-1	CHV/0194	Canine	UK	NC_030117.1	(Papageorgiou et al., 2016)				

Table 2

The number of unique synonymous amino acid substitutions and unique nonsynonymous amino acid substitutions across all isolates sequenced for this study. Individual nonsynonymous substitutions are also shown in the column on the right.

Gene	Gene Product	Number Unique Synonymous Substitutions	Number Unique Nonsynonymous Substitutions	Nonsynonymous Substitutions
CIRC	myristylated tegument protein CIRC	2	0	none
ICP0	ubiquitin E3 ligase ICP0	1	1	Thr479Ser
ICP4	transcriptional regulator ICP4	0	0	none
UL1	envelope glycoprotein L	0	1	Thr111Ile
UL10	envelope glycoprotein M	1	1	Val142Ile
UL11	myristylated tegument protein	0	0	none
UL12	deoxyribonuclease	1	0	none
UL13	tegument serine/threonine protein kinase	1	0	none
UL14	tegument protein UL14	0	2	Tyr167His, Ser25Pro
UL15	DNA packaging terminase subunit 1	2	4	Thr426Pro, Ala4Gly, His471Gln, Pro614Gln
UL16	tegument protein UL16	0	0	none
UL17	DNA packaging tegument protein UL17	0	0	none
UL18	capsid triplex subunit 2	0	0	none
UL19	major capsid protein	3	2	Arg333Leu, Asp14Glu
UL20	envelope protein UL20	2	1	none
UL21	tegument protein UL21	0	1	Ala265Val
UL22	envelope glycoprotein H	0	1	Asp723Asn
UL23	thymidine kinase	0	1	Thr20Ile
UL24	nuclear protein UL24	0	0	none
UL25	DNA packaging tegument protein UL25	0	0	none
UL26	capsid maturation protease	0	0	none
UL26.5	capsid scaffold protein	0	0	none
UL27	envelope glycoprotein B	0	3	Pro360Thr, Val627Leu, Gly940Ser
UL28	DNA packaging terminase subunit 2	2	2	Pro427Gln, Gly300Ala
UL29	single-stranded DNA-binding protein	2	2	Ser1089Pro, Val483Ile
UL3	nuclear protein UL3	0	0	none
UL3.5	protein V57	0	2	Glu162Gly, Pro45Leu
UL30	DNA polymerase catalytic subunit	0	1	Ile153Thr
UL31	nuclear egress lamina protein	0	1	Arg53Gln
UL32	DNA packaging protein UL32	2	0	none
UL33	DNA packaging protein UL33	0	1	Phe51Leu
UL34	nuclear egress membrane protein	1	0	none
UL35	small capsid protein	0	1	Ser3Arg

Gene	Gene Product	Number Unique Synonymous Substitutions	Number Unique Nonsynonymous Substitutions	Nonsynonymous Substitutions
UL36	large tegument protein	3	5	Asn2936_Val2937del, Pro2838Ser, Arg3006His, Asp422Glu, Thr291Ile
UL37	tegument protein UL37	1	0	none
UL38	capsid triplex subunit 1	1	2	Ile277Met, Gly55Asp
UL39	ribonucleotide reductase subunit 1	0	0	none
UL4	nuclear protein UL4	0	0	none
UL40	ribonucleotide reductase subunit 2	0	2	Val66Ile, Pro8Leu
UL41	tegument host shutoff protein	2	0	none
UL42	DNA polymerase processivity subunit	1	0	none
UL43	envelope protein UL43	0	0	none
UL44	envelope glycoprotein C	0	1	Lys133Glu
UL45	membrane protein UL45	0	0	none
UL46	tegument protein VP11/12	0	1	Ser666Pro
UL47	tegument protein VP13/14	1	1	Leu132Ser
UL48	transactivating tegument protein VP16	0	1	Leu132Ser
UL49	tegument protein VP22	0	0	none
UL49.5	envelope glycoprotein N	0	0	none
UL5	helicase-primase helicase subunit	2	1	Gly136Ser
UL50	deoxyuridine triphosphatase	0	0	none
UL51	tegument protein UL51	0	0	none
UL52	helicase-primase primase subunit	0	2	Tyr484Cys, Arg208Lys
UL53	envelope glycoprotein K	0	0	none
UL54	multifunctional expression regulator	0	0	none
UL55	nuclear protein UL55	0	4	Ile78Met, Arg93Gly, Arg108Ser, Pro116Ser
UL56	membrane protein UL56	0	0	none
UL6	capsid portal protein	2	0	none
UL7	tegument protein UL7	0	0	none
UL8	helicase-primase subunit	1	0	none
UL9	DNA replication origin-binding helicase	2	1	Val637Met
US1	regulatory protein ICP22	0	0	none
US10	virion protein US10	0	0	none
US2	virion protein US2	0	1	His46Tyr
US3	serine/threonine protein kinase US3	0	0	none
US4	envelope glycoprotein G	0	1	Ser326Asn
US6	envelope glycoprotein D	0	0	none
US7	envelope glycoprotein I	1	1	Met165Thr
US8	envelope glycoprotein E	0	2	Ser458Pro, Arg423Cys
US8A	membrane protein US8A	0	0	none

Gene	Gene Product	Number Unique Synonymous Substitutions	Number Unique Nonsynonymous Substitutions	Nonsynonymous Substitutions
US9	membrane protein US9	1	0	none
V1	membrane protein V1	0	1	Phe126fs
V32	protein V32	0	0	none